Diabetes, Metabolic Syndrome and Obesity

Dovepress
Taylor & Francis Group

Open Access Full Text Article

ORIGINAL RESEARCH

Protective Effect of Semaglutide on Obesity-Induced Renal Disease and Obesity-Induced Kidney Renal Clear Cell Carcinoma

Shuqi Wang[1,2], Mengmeng Zhang[1,2], Xiaoman Yang[1,2], Shuchun Chen[1–3]

[1]Department of Internal Medicine, Hebei Medical University, Shijiazhuang, People's Republic of China; [2]Department of Endocrinology, Hebei General Hospital, Shijiazhuang, People's Republic of China; [3]Key Laboratory of Metabolic Diseases in Hebei Province, Shijiazhuang, People's Republic of China

Correspondence: Shuchun Chen, Department of Endocrinology, Hebei General Hospital, Shijiazhuang, People's Republic of China, Tel/Fax +86 31185988406, Email chenshuc2014@163.com

Purpose: Proteomics was used to study the effect of semaglutide on the expression of renal protein in obese mice, and looking for proteins that could improve the prognosis of Kidney Renal Clear Cell Carcinoma (KIRC).

Materials and Methods: Thirty-six mice were randomly divided into normal-fat diet group (NFD), high-fat diet group (HFD), high-fat diet plus semaglutide intervention group (HS). Collected mice serum, urine, kidney tissue samples, and detected urinary protein/creatinine, blood glucose, blood lipid, inflammation, oxidative stress and other related indicators. Different staining methods were used to analyze the pathological changes of mice's kidneys. Liquid chromatography-tandem mass spectrometry mass spectrometry (LC-MS /MS) analysis was used to analyze the total protein in the kidneys of mice. Finally, bioinformatics technology was used to analyze significantly different expressed proteins (DEPs).

Results: The mechanism of semaglutide protecting the kidneys were related to oxidative phosphorylation, PPAR signaling pathway, thiamine, butyric acid and tryptophan metabolism pathways. Moreover, semaglutide could significantly increase the expression of Man1a1 and Ntn4 in the kidneys of mice, while the high-expression of Man1a1 and Ntn4 in KIRC population had a better overall survival rate.

Conclusion: Semaglutide could regulate the development of KIRC by up-adjusting the expression of Man1a1 and Ntn4.

Keywords: obesity, semaglutide, kidney renal clear cell carcinoma, proteomics

Introduction

Obesity is a major challenge facing the world. It has different effects on human metabolism, endocrine, immunity, psychology and behavior. With the increasing prevalence of obesity worldwide, obesity has become a major public health problem.[1] Studies have shown that obesity is an important factor leading to the incidence of cardiovascular diseases, diabetes, musculoskeletal diseases, neurodegenerative diseases, etc., and is closely related to the increase in the overall cause mortality rate of patients. At least 3 million people worldwide die from obesity-related diseases every year.[2] What's more worrying is that obesity increases the risk of cancer. Mendel's randomized research supports obesity leading to a variety of cancers, especially 13 cancers related to the digestive tract, urinary system and reproductive system. However, obesity is also the second largest preventable cancer factor after smoking. Obesity is closely related to the occurrence of cancer.[3]

As one of the most common malignant tumors of the urinary system, the incidence of renal carcinoma is increasing year by year. Cohort studies show that BMI and WC are positively associated with the risk of renal carcinoma, and systemic obesity and abdominal obesity are important risk factors for renal carcinoma.[4] For patients who have undergone weight loss surgery, the first hospitalization rate of renal carcinoma is significantly lower than those who have

Received: 29 September 2024
Accepted: 11 March 2025
Published: 19 March 2025

not performed weight loss surgery.[5] Weight control in obese patients is of great significance to reducing the incidence of renal carcinoma. Semaglutide is a typical weekly preparation representative drug in glucagon-like peptide 1 (GLP-1) receptor agonists, reduces patients' blood glucose through the "Incretin effect" and has also become a new generation of diet pills because of its effect of inhibiting appetite. Previous animal experiments have found that semaglutide can benefit the heart, blood vessels, liver, skeletal muscle, cognitive function of mice by improving glycolipid metabolism, improving inflammation and oxidative stress levels.[6–10] At the same time, semaglutide can reverse kidney damage caused by obesity through NAD+ metabolism and insulin resistance-related metabolism.[11] Semaglutide has become the preferred treatment drug for obesity-related metabolic syndrome because of its significant multi-organ protection and safety.

Although the research of semaglutide is deeper and deeper, little is known about the impact of semaglutide on cancer, especially for KIRC. In order to further explore the effect of semaglutide on obesity-induced KIRC, this study used proteomic analysis methods and bioinformatics to screen proteins related to KIRC, revealing the molecular mechanism of semaglutide regulating the KIRC.

Materials and Methods

Animals, Reagents and Materials

Five-week-old male C57BL/6J mice, F02-002 normal-fat feed (10% total calories of fat), D12492 high-fat feed (60% total calories of fat) were purchased from SPF Biotechnology Co., Ltd (Beijing, China). Semaglutide was provided by Novo Nordisk, Denmark. Urine protein test kit and urine creatinine test kit were purchased from Elabscience (Wuhan, China). The lipid test kit and malondialdehyde (MDA) kits were purchased from Nanjing Construction Bioengineering Research Institute Co., Ltd (Nanjing, China). Superoxide dismutase (SOD) kits, tumor necrosis factor-α (TNF-α) kits, interleukin-6 (IL-6) kits were purchased from bioswamp (Wuhan, China). Roche's blood glucose meter was purchased from Roche.

Animal Treatment and Research Design

Placed 5-week-old mice in an animal room suitable for an environment (temperature 22 ± 2°C, humidity of 55 ± 10%, circulation 12 h day and night), regularly changed the padding, eat and drink water freely. After a week of adaptive feeding of ordinary feed, mice were randomly divided into three groups, namely, normal-fat diet group (NFD, n = 12), high-fat diet group (HFD, n = 12), high-fat diet plus semaglutide intervention group (HS, n = 12). Among them, after feeding high-fat feed for 14 weeks, the mice in the HS group regularly intraperitoneal injection semaglutide 30 nmol/kg/d every day.[11] The NFD and HFD groups continued to give normal-fat feed and high-fat feed, respectively, and injected the equivalent amount of saline every day. The total duration of the intervention was 22 weeks, and the weight of 3 groups of mice was measured every week. Measured the body length of mice before the end of the experiment and calculated Lee's index. Lee's index= (body weight (g)×1000)$^{1/3}$/body length (cm).

Glucose Tolerance Tests

The blood sugar of mice was measured with a Roche blood glucose meter. After 12 hours of fasting, fasting blood glucose is measured by tail vein blood collection, and then 20% high glucose 2g/kg was injected into the abdominal cavity. After injecting high sugar, mouse tail vein blood was collected for 15 minutes, 30 minutes, 60 minutes, 90 minutes and 120 minutes to measure blood sugar and record. Calculated the area under the curve of the intraperitoneal glucose tolerance test (IPGTT AUC). IPGTT AUC = 0.5*(Bg 0 min + Bg 30 min) /2 + 0.5*(Bg 30 min + Bg 60 min)/2 + 1*(Bg 60 min + Bg 120 min)/2, B Glucose was the blood sugar value at each point in time.

Collection and Treatment of Urine and Blood Samples

After 22 weeks of intervention, collected mouse urine in a metabolic cage, and take out the upper liquid after centrifugation (2000 rpm, 10 min), then used the kit to measure urine protein and creatinine in mice. After the mice were fasted for 12 hours, 1% pentobarbital sodium (60 mg/kg) was injected into the abdominal cavity to anesthetize the

mice, and the blood was collected from the inner canthus vein. After blood was collected, the mouse was immediately executed by cervical dislocation. The collected blood samples were rested for 60 minutes, centrifugated (4°C, 3500rpm, 15 min) and used fully automatic biochemical analyzer determined serum total cholesterol (TC), low-density lipoprotein cholesterol (LDL-C) and MDA.

Determination of Kidney Tissue SOD, IL-6, TNF-α

Dissection of the mouse's abdominal cavity, removed the bilateral kidneys, and immediately saved them in the −80°C refrigerator. We randomly selected three left kidney tissues. Renal tissue was lysed with lysate, and centrifugation (4°C, 3000 rpm, 15 min). SOD, TNF-α and IL-6 were determined by enzyme-linked immunosorbent assay method (ELISA) in the kidney tissue of mice. All operations are carried out in strict accordance with the manufacturer's instructions.

Kidney Pathology Detection

Each group randomly selected 3 left kidney samples for fixation in 4% polyformaldehyde. After 48 hours of fixation at room temperature, gradient alcohol dehydration, xylene transparent, paraffin burial and slicing. The pathological changes of the kidneys were analyzed by HE staining, PAS staining and Masson staining. Each group randomly selected 10 fields to calculate the length of the glomerular blood vessel to the urine pole and glomerular area. Each group randomly selected 10 fields to evaluate renal tubular injury. Tubular damage was defined as renal tubular brush edge shedding, renal tubular swelling or atrophy, and renal tubular type. According to the percentage of damaged renal tubules in the area under the field of vision: normal is 0 points, the damaged area accounts for less than 25% of the field of vision is 1 point, 25%–50% is 2 points, 50%–75% is 3 points, and 75%–100% is 4 points. Each group randomly selected 10 fields to calculate the percentage of the positive field of the total area under Masson staining. The kidney tissue was fixed with 4% polyformaldehyde and made into a frozen section. It was stained with Oil Red O solution. After multiple washings of PBS, the nucleus was reversed with oxylin to observe the renal lipid deposition area. Data analysis used Image-Pro Plus software.

Preparation of Proteomics Samples

Four mouse left kidney samples were selected in each group. About 20–50 mg wet-weight tissue for each sample was lysed in TCEP buffer (2% deoxycholic acid sodium salt, 40 mm 2-Chloroacetamide, 100 mm Tris-HCl, 10 mm Tris (2-chloroethyl) phosphate, 1 mm PFSM, 1 mm Cocktail, pH 8.5) supplemented with protease inhibitors and phosphatase at 99°C for 30 min. After cooling to room temperature, trypsin (Promega, Madison, WI, USA, #V5280) was added and digested for 18 h at 37°C. 10% formic acid was added and vortex for 3 min, followed by sedimentation for 5 min (12,000 g). Next, a new 1.5 mL tube with extraction buffer (0.1% formic acid in 50% acetonitrile) was used to extract the supernatant (vortex for 3 min, followed by 12,000 g of sedimentation for 5 min). Collected supernatant and dried using a speed-vac. 20 μg protein for each sample were mixed with 2X loading buffer respectively and boiled for 5 min. The proteins were separated on SDS-PAGE gel (constant current 120 V, 60 min). Protein bands were visualized by Coomassie Blue R-250 staining.

Nano-LC–MS/MS Analysis

For the proteome profiling samples, peptides were analyzed on an OE480 hybrid Quadrupole-Orbitrap Mass Spectrometer (Thermo Fisher Scientific) coupled with a high-performance liquid chromatography system (EASY nLC 1200, Thermo Fisher Scientific). Dried peptide samples re-dissolved in Solvent A (0.1% formic acid in water) were loaded onto a 2-cm self-packed trap column (100 μm inner diameter, Dr. Maisch GmbH) using Solvent A and separated on a 150-μm-inner-diameter column with a length of 15 cm (1.9 μm ReproSil-Pur C18-AQ beads, Dr. Maisch GmbH) over a 120-min gradient (Solvent A: 0.1% formic acid in water; Solvent B: 0.1% formic acid in 80% ACN) at a constant flow rate of 600 nL/min (0–120 min, 0 min, 4% B; 0–8 min, 4–15% B; 8–100 min, 15–35% B; 100–110 min, 30–50% B; 110–111 min, 50–100% B; 111–120 min, 100% B). Eluted peptides were ionized at 2.4 kV and introduced into the mass spectrometer. Mass spectrometry was performed in data-dependent acquisition mode. For the MS1 Spectra full scan, ions with m/z ranging from 300 to 1400 were acquired by an Orbitrap mass analyzer at a high resolution of 120,000. The

automatic gain control (AGC) target value was set to 3E+06. The maximal ion injection time was 80 ms. MS2 spectral acquisition was performed in a rapid speed mode with 1s cycletime. Precursor ions were selected and fragmented with higher energy collision dissociation (HCD) with a normalized collision energy of 30%. Fragment ions were analyzed by an Orbitrap mass analyzer at the resolution of 7500, with an AGC target at 5E+04. The maximal ion injection time of MS2 was 22 ms. Peptides that triggered MS/MS scans were dynamically excluded from further MS/MS scans for 40 s. The coefficient of variation (CV) values on FAIMS were −45V and −65V.

Data Analysis

The obtained raw data were analyzed, and iProteome one-stop data analysis cloud platform was used for qualitative and quantitative analysis. Peptide FDR ≤ 0.01 is used as the screening criterion in data qualitative analysis.

GO and KEGG Analyses

Screened the protein of FC≥1.5 or FC≤0.67, pValue <0.05, and carry out GO functional enrichment analysis (http://www.ebi.ac.uk/goa/) and KEGG pathway enrichment analysis (https://www.kegg.jp/kegg/mapper/) for the screened DEPs. The enrichment analysis was accurately tested by Fisher, and the difference of P<0.05 was statistically significant.

Diagnostic Value and Prognosis Analysis of DEPs for KIRC

The Gepia2 database (http://gepia2.cancer-pku.cn) was used to analyze DEPs.

Proteins in the HFD/NFD mice with the same expression trend in KIRC tissue/normal tissue were screened. The screened DEPs were introduced into the pan-cancer analysis tool sangerbox (http://sangerbox.com/login.html), used the KIRC database to conduct ROC curve analysis of DEPs and detected the diagnostic value of DEPs for KIRC. Subsequently, the Gepia2 database was used to analyze the survival prognosis value of DEPs for KIRC.

Statistical Analysis

Statistical analysis of the data was performed using SPSS 21.0 software, while graphical representations were generated using GraphPad Prism 8.0.2 and micro-shengxin online tool (https://www.bioinformatics.com.cn). Comparisons were performed by one-way analysis of variance (ANOVA). P < 0.05 was statistically significant for the difference.

Results

Semaglutide Significantly Reduced the Weight of Obese Mice and Improved Glycolipid Metabolism and Kidney Damage, Inflammation and Oxidative Stress in Mice

Weight Changed in Mice

There were no significant difference in the weight of the three groups of mice at the age of 6 weeks. After 14 weeks of high-fat intervention, the weight of HFD, HS mice were significantly higher than that of NFD mice (P < 0.001), indicating that the obesity model was successful. Subsequently, the HS group gave semaglutide intervention, and the other two groups gave an equal amount of physiological saline intervention. At the end of the experiment, the weight of HS mice decreased significantly compared with that of HFD mice (P < 0.001), and there was no significant difference from that of NFD mice (Figure 1A). Lee's index of HFD mice was significantly higher than that of NFD mice, and Lee's index of HS mice was significantly lower than that of HFD mice (P < 0.05) (Figure 1B).

Glycolipid Metabolism Changed in Mice

The glucose tolerance experiment showed that the blood glucose of HFD mice was higher than other groups of mice at 15 min, 30 min, 60 min, 90 min, and 120 min (Figure 1C). Quantitative analysis showed IPGTT AUC of HFD mice was significantly higher than NFD mice, while IPGTT AUC of HS mice decreased significantly lower than HFD mice (P < 0.05) (Figure 1D).

The TC levels of HFD mice were significantly higher than that of NFD mice, TC in HS mice had a downward trend compared with HFD mice, but the difference was not significantly statistically significant (Figure 1E). The LDL-C levels

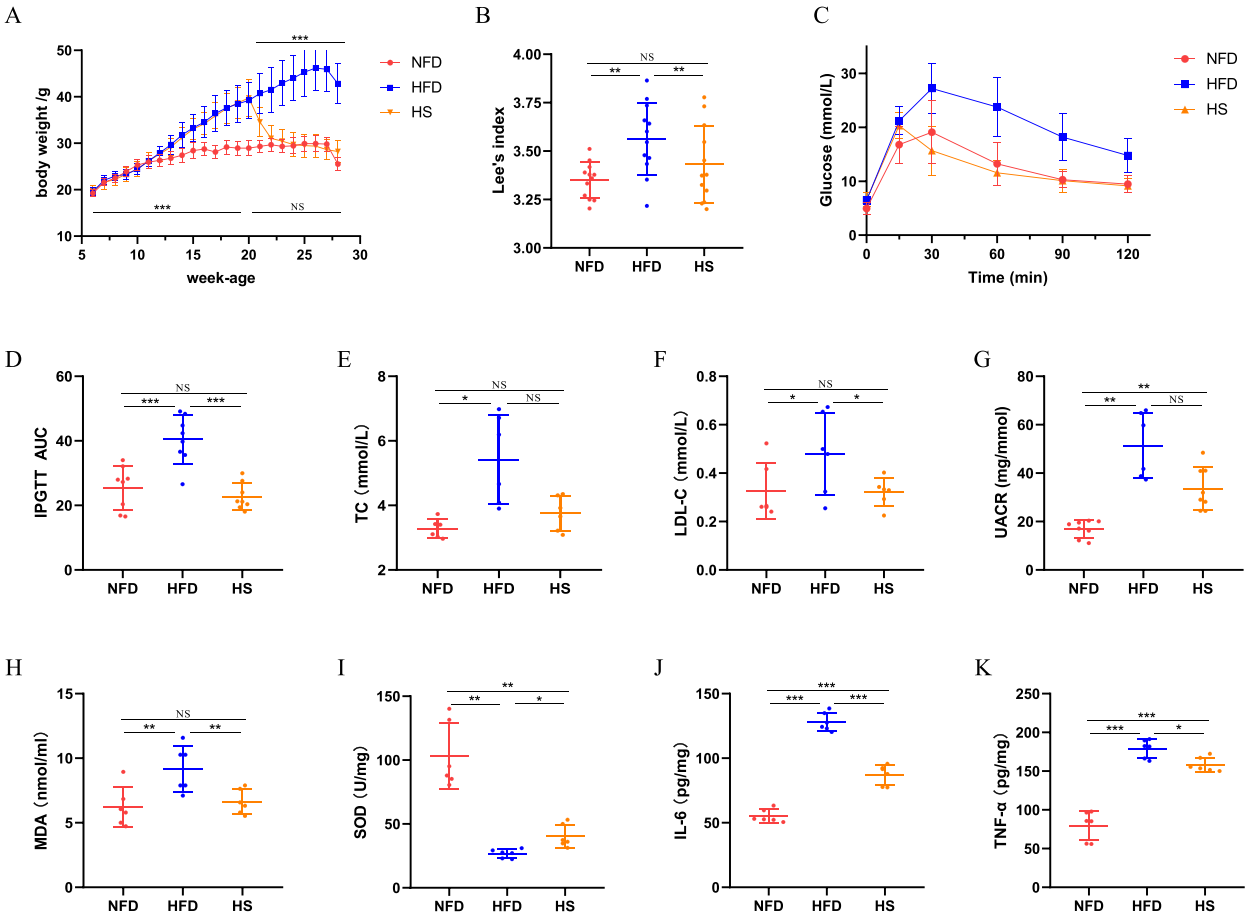

Figure 1 Changes of weight (**A**), Lee's index (**B**), Glucose (**C**), IPGTT AUC (**D**), TC (**E**), LDL-C (**F**), UACR (**G**), MDA (**H**), SOD (**I**), IL-6 (**J**) and TNF-α (**K**) in mice.
Notes: *Denotes significance at a P value of <0.05, **Denotes significance at a P value of <0.01, ***Denotes significance at a P value of <0.001, NS indicates that the difference has no significant significance.
Abbreviations: NFD, normal-fat diet group; HFD, high-fat diet group; HS, high-fat diet plus semaglutide intervention group; IPGTT AUC, the area under the curve of the intraperitoneal glucose tolerance test; TC, total cholesterol; LDL-C, low-density lipoprotein cholesterol; UACR, urinary protein/creatinine; MDA, malondialdehyde; SOD, Superoxide dismutase; TNF-α, tumor necrosis factor-α; IL-6, interleukin-6.

of HFD mice were significantly higher than those of NFD mice, LDL-C of HS mice was significantly lower than HFD mice ($P < 0.05$) (Figure 1F).

Kidney Injury Changed in Mice

Detected urine protein and urinary creatinine levels in mice and calculated urinary protein/creatinine (UACR). It was found that the UACR levels of HFD mice were significantly higher than NFD mice ($P < 0.05$), and the UACR levels of HS mice had a downward trend compared with HFD mice, but the difference was not significantly statistically significant (Figure 1G).

Inflammation and Oxidative Stress Changed in Mice

The serum MDA levels of HFD mice were significantly higher than NFD mice, serum MDA levels of HS mice were significantly lower than HFD mice ($P < 0.05$) (Figure 1H). The SOD levels of kidney tissue of HFD mice were significantly lower than NFD mice, and the SOD levels of HS mice were significantly higher than HCD mice ($P < 0.05$) (Figure 1I). The renal tissue IL-6 and TNF-α levels of HFD mice were significantly higher than NFD mice, the renal tissue IL-6 and TNF-α levels of HS mice were significantly lower than that of HFD mice, and the differences were statistically significant ($P < 0.05$) (Figure 1J and K).

https://doi.org/10.2147/DMSO.S498447

Semaglutide Significantly Improved Kidney Pathological Changes in Obese Mice

HE Staining

HE staining indicated that the glomerular matrix of HFD mice had mild hyperplasia, the vacuolar denatured of renal tubular epithelial cells was obvious, the cells were swollen. But the glomerular and tubular lesions of HS mice were lighter than HFD mice (Figure 2A). Quantitative measurements found that the glomerular diameter of HFD mice was significantly higher than NFD mice, the glomerular diameter of HS mice was significantly lower than HFD mice ($P < 0.05$) (Figure 2E). The renal tubular injury index of HFD mice was significantly higher than NFD mice ($P < 0.05$), the tubular injury index of HS mice had a downward trend compared with HFD mice, but the difference was not statistically significant (Figure 2G).

PAS Staining

PAS staining observed that the glomerular area of HFD mice increased significantly compared with NFD mice, and the glomerular mesangial cells hyperplasia, while the glomerulus of HS mice did not see obvious abnormalities (Figure 2B). Quantitative analysis found that the glomerular area of HFD mice was significantly higher than NFD mice, and the glomerular area of HS mice was significantly lower than HFD mice (Figure 2F).

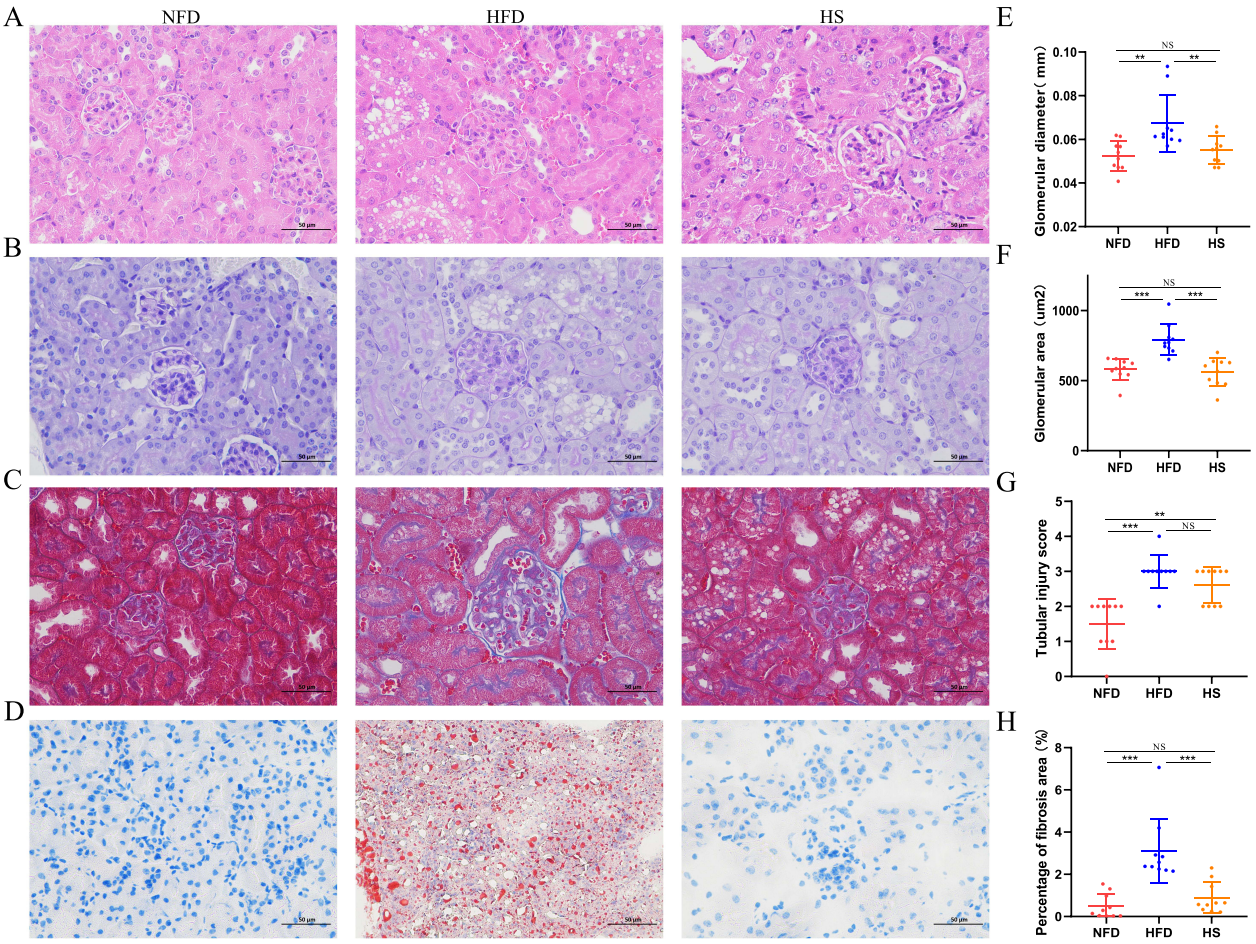

Figure 2 Changes of HE staining (**A**), PAS staining (**B**), Masson staining (**C**), oil red O staining (**D**), glomerular diameter (**E**), glomerular area (**F**), tubular injury score (**G**) and percentage of fibrosis area (**H**) in mice.

Notes: *Denotes significance at a P value of <0.05, **Denotes significance at a P value of <0.01, ***Denotes significance at a P value of <0.001, NS indicates that the difference has no significant significance.

Abbreviations: NFD, normal-fat diet group; HFD, high-fat diet group; HS, high-fat diet plus semaglutide intervention group.

Masson Staining

Renal interstitial fibrosis was observed in HFD mice in Masson staining. The qualitative analysis of the area of interstitial fibrosis in HFD mice was significantly higher than NFD mice, while the percentage of renal interstitial fibrosis area in HS mice was significantly lower than that of HFD mice ($P < 0.05$) (Figure 2C and H).

Oil Red O Staining

Under the optical microscope, the lipid deposition of HFD mice was more obvious than NFD mice, and the lipid deposition of HS mice was less than HFD mice (Figure 2D).

Kidney Proteomics Analysis of Mice

Identification of DEPs in Mice

According to the DEPs screening criteria, a total of 271 DEPs were identified in the kidney tissue of the HFD/NFD mice, of which 105 proteins were upregulated and 166 proteins were lowered. A total of 1127 DEPs were identified in the kidneys of the HS/HFD mice, of which 997 proteins were upregulated and 130 proteins were lowered. Differential expression analysis and cluster analysis of DEPs were presented with volcanic and thermal maps (Figure 3A and B).

GO and KEGG Enrichment Analysis of Reverse Expression of Differential Proteins

Comparing the DEPs of the HFD/NFD mice and the HS/HFD mice, a total of 119 DEPs were screened to show the reverse changes to the induced obesity group after the intervention of semaglutide. The GO function enrichment analysis of 119 DEPs showed that in terms of biological processes (BP), DEPs were mainly involved in carboxylic acid transport, monovalent inorganic cation transport, protein catabolic process, small molecule metabolic process, sulfur compound metabolic process (Figure 4A). In terms of molecular function (MF), DEPs were related to active transmembrane transporter activity, flavin adenine dinucleotide binding, phospholipid binding, structural constituent of ribosome, sulfur compound binding (Figure 4B). In cell components (CC), DEPs mainly distributed coated vesicle, mitochondrial inner membrane, mitochondrial matrix, organelle inner membrane, ribosomal subunit (Figure 4C). KEGG pathway enrichment analysis was carried out on 119 DEPs, and the results showed that the main enrichment pathways were Butanoate metabolism, Oxidative phosphorylation, PPAR signaling pathway, Thiamine metabolism, Tryptophan metabolism (Figure 4D).

Analyzed the Diagnostic and Prognostic Value of DEPs in KIRC by Bioinformatics Database

Used Gepia2 database to analyze the DEPs. It was screened out that Man1a1 and Ntn4 were lowered in the HFD/NFD group mice and up in the HS/HFD mice, while Man1a1 and Ntn4 were lowered in KIRC tissue/normal tissue ($P < 0.05$) (Figure 5A-C). The screened DEPs were introduced into the pan-cancer analysis tool, and the ROC curve of KIRC was analyzed. It was found the low-expression Man1a1 and Ntn4 had good diagnostic value for KIRC (Table 1, Figure 5D). Survival analysis suggested that people with high expression of Man1a1 and Ntn4 had a better overall survival rate ($P < 0.05$) (Figure 5E and F).

Discussion

Renal carcinoma is the 13th most common cancer in the world, accounting for 2.4% of all cancers. In 2020, there were about 431,288 new cases of renal carcinoma worldwide.[12] A large amount of clinical data support that obesity is associated with the risk of renal carcinoma. Research shows that for every $1kg/m^2$ increase in BMI, the risk of renal carcinoma increases by 4%, and high BMI leads to at least 26% of renal carcinoma events.[13] Renal carcinoma seriously endangers human health and life safety. More than 131,000 people die from renal carcinoma every year, analysis of the global renal carcinoma burden attribution shows that body mass index and smoking account for 18.5% and 16.6%, respectively.[14] According to South Korea's National Health Insurance Service (NHIS) in the past 13 years, the total cost of renal carcinoma caused by overweight or obesity was $1.6 trillion in male patients alone.[15] Obesity can induce cancer through a variety of mechanisms. Obesity keeps the body in a state of chronic low-degree inflammation for a long time,

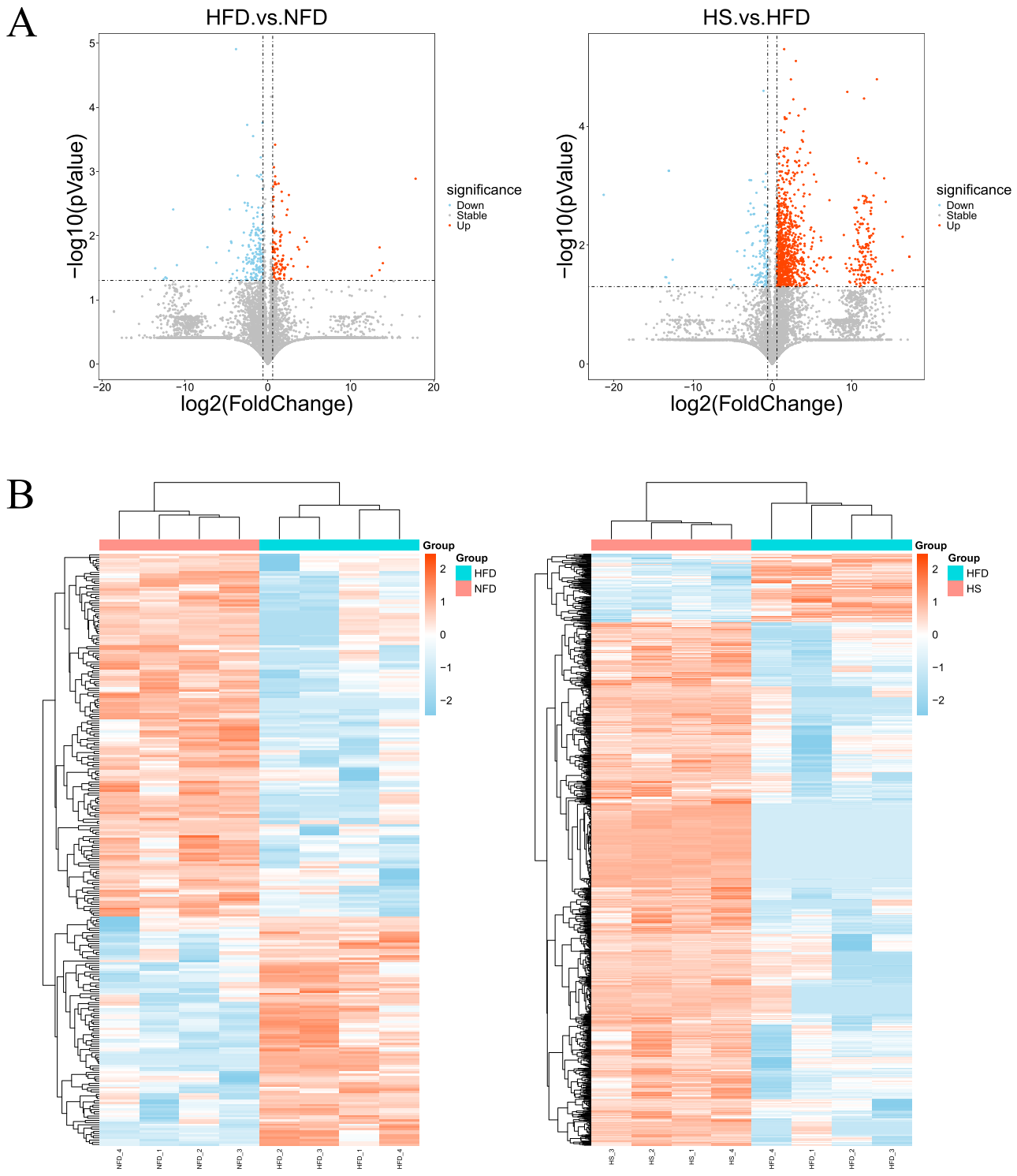

Figure 3 Identification of mice kidney proteomics DEPs.
Notes: Differential expression volcano map analysis of DEPs (**A**), Cluster heat map analysis of DEPs (**B**).
Abbreviations: NFD, normal-fat diet group; HFD, high-fat diet group; HS, high-fat diet plus semaglutide intervention group.

and adipose tissue produces a series of pro-inflammatory factors that constantly aggravate the damage of cell DNA. In particular, TNF-α can stimulate the growth, proliferation, invasion and metastasis of cancer cells, which is closely related to the occurrence and development of cancer.[16] In our study, we found that the renal tissue TNF-α levels of HFD mice

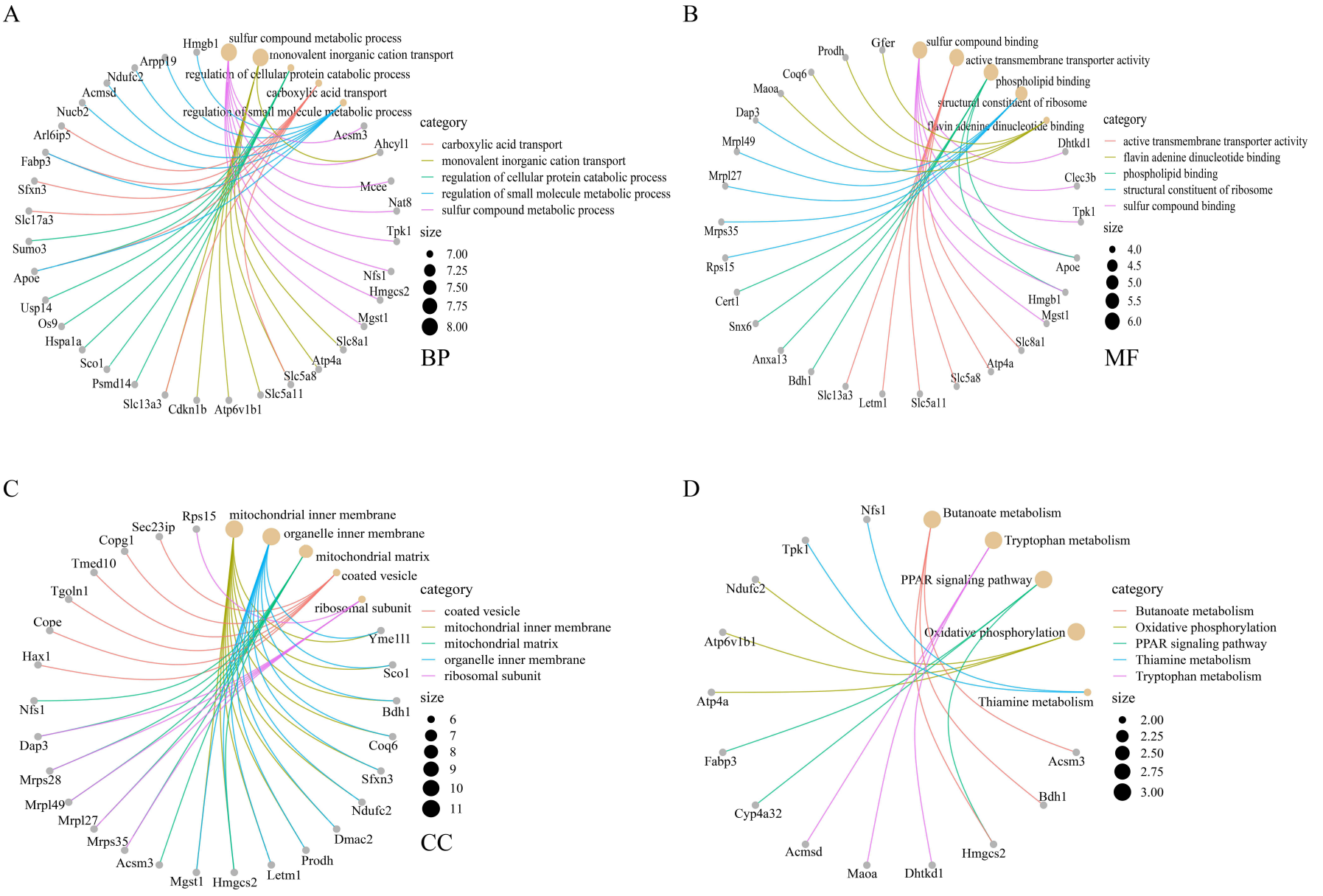

Figure 4 Enrichment analysis of DEPs.

Notes: Biological process analysis of the reverse expression DEPs in GO (**A**), Molecular function analysis of the reverse expression DEPs in GO (**B**), Cell components analysis of the reverse expression DEPs in GO (**C**), KEGG analysis of the reverse expression DEPs (**D**).

https://doi.org/10.2147/DMSO.S498447

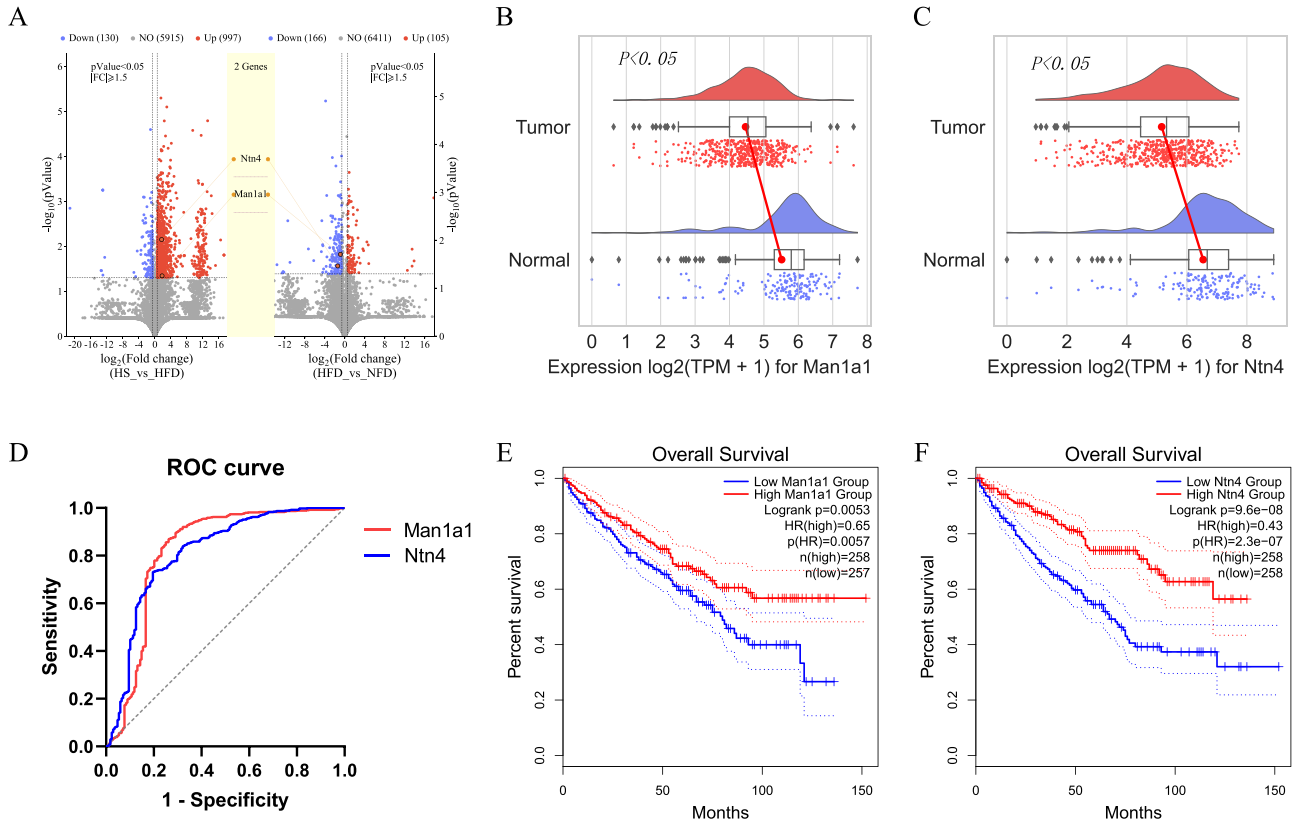

Figure 5 The diagnostic and prognostic value of DEPs to KIRC.

Notes: Reverse expression of DEPs in renal proteomics (**A**), Expression of Man1a1 in KIRC (**B**), Expression of Ntn4 in KIRC (**C**), Diagnostic value of DEPs to KIRC (**D**), Man1a1's analysis of survival in KIRC (**E**), Ntn4's analysis of survival in KIRC (**F**).

Abbreviations: Man1a1, Mannosyl-oligosaccharide 1.2-alpha-mannosidase IA; Ntn4, Netrin-4, NFD, normal-fat diet group; HFD, high-fat diet group; HS, high-fat diet plus semaglutide intervention group.

was significantly higher than NFD mice, and other inflammatory and oxidative stress factors related to DNA damage were also significantly increased in HFD mice. When obese, insulin function is reduced, insulin resistance is increased, insulin and insulin-like growth factor (IGF) levels in serum increase. Excessive IGF and insulin-like growth factor-binding protein (IGFBP) can promote cell cycle progression and inhibit apoptosis, thus increasing cancer cell activity.[17] Genetics has found that the obesity gene (FTO) is the most closely related gene associated with increased body mass index among obesity-related genes, at the same time, FTO can be used as RNA m6A demethylase to regulate cancer cells, resulting in high expression in a variety of cancerous tissues.[18] Mendel's randomized research shows that the FTO A allele is closely related to the increased risk of renal carcinoma (OR = 1.44, CI 1.09–1.90).[19] Therefore, weight loss is of great significance for controlling the occurrence and development of renal carcinoma.

Semaglutide can reduce weight by regulating glucose steady-state, insulin secretion, energy consumption, lipid metabolism and appetite.[20] In our experiment, the weight of HS mice was significantly lower than that of HFD mice, but there was no significant difference from NFD mice. After the application of semaglutide, the kidney damage,

Table 1 DEPs ROC Curve Analysis of KIRC

Variable	AUC	P-value	95% (CI)
Man1a1	0.818	P<0.001	0.771–0.865
Ntn4	0.811	P<0.001	0.769–0.853

Abbreviations: Man1a1, Mannosyl-oligosaccharide 1,2-alpha-mannosidase IA; Ntn4, Netrin-4.

glycolipid metabolism levels, inflammation and oxidative stress in obese mice induced by a high-fat diet were significantly improved. Pathological sections suggested that semaglutide intervention can reduce glomerular and tubular damage, and these results were also consistent with previous experimental results.[11] We identified and screened the renal protein expression in mice, and found that a total of 119 DEPs showed reverse changes to the inducing obesity group after semaglutide intervention, and the main enrichment pathways were closely related to oxidative phosphorylation, PPAR signaling pathways, thiamine, butyric acid and tryptophan metabolism.

Oxidative phosphorylation generates ATP in the process of electron transfer of respiratory chain. Mitochondrial protein sequence variation is found in the genome of obese and diabetic mice, resulting in mitochondrial protein synthesis defects, reduced level expression of oxidative phosphorylation complex, and blocked phosphorylation process, resulting in mouse obesity and insulin resistance phenotype.[21] Single-cell transcriptome analysis of patients with obesity-related glomerulopathy also suggested that the oxidative phosphorylation pathway was highly enriched in KEGG.[22] The role of PPAR signaling pathway in diabetes, cancer, cardiovascular disease and other chronic diseases has been fully proven, and plays an important role in regulating glycolipid metabolism and energy homeostasis.[23–25] PPARβ/δ can uptune mitochondrial function, and in cancerous tissues, it can promote metabolic reprogramming from glucose degradation to lipid metabolism and glutamine metabolism, which can help cancer cells survive and proliferate when energy is scarce.[26] Previous studies have found that butyric acid is an important intermediary for the metabolic health of intestinal flora and hosts, butyric acid metabolism is closely related to inhibiting obesity, anti-inflammation and maintaining glucose homeostasis.[27] The high-fat diet affects macrophage polarization by inducing intestinal microbial dysplasia and inhibiting butyric acid metabolism, driving the occurrence of colitis-related tumors.[28] Thiamine can be used as a coenzyme to participate in citric acid circulation. In animal experiments, it has been found that thiamine treatment can improve steat degeneration in the liver, heart and skeletal muscle, reduce urine volume and urinary protein excretion in diabetic rats, reduce the thickness of glomerular basal membrane and renal interstitial fibrosis, and significantly improve renal function.[29] Tryptophan metabolism produces a variety of active compounds, participating in inflammation, metabolism, immune response, neurological function and other biological approaches. The tryptophan-kynurenine pathway can be involved in immune activation and inflammatory response, regulating obesity and insulin resistance, and its metabolites are associated with an increased risk of type 2 diabetes.[30] A cohort study of obese children also supported a significant increase in plasma tryptophan and kynurenine concentrations in children in the early stage of obesity and diabetes, and were negatively associated with adiponectin.[31] Proteomics enrichment analysis showed that the enrichment pathway of semaglutide's intervention in obesity is closely related to glycolipid metabolism, inflammation and insulin resistance, which is also supported by the serum and tissue detection indicators and kidney pathological results in our experimental mice.

In order to clarify the molecular mechanism of the action of semaglutide on renal carcinoma, we further conducted bioinformatics screening of these 119 DEPs and found that the Man1a1 and Ntn4 proteins decreased in the HFD/NFD mice and rose in the HS/HFD group. In the renal carcinoma database, these three proteins are low-expressed in KIRC, and had strong diagnostic value for KIRC. Perhaps, Man1a1 and Ntn4 can become intervention targets for semaglutide for KIRC.

Glycosylation is an important protein modification method that occurs in the endoplasmic reticulum and the Golgi body, which has an important impact on protein stability, molecular recognition, signaling, etc. Studies have found that abnormalities in glycosylation can be used as a sign of cancer.[32] In breast cancer, ovarian cancer, bile duct cancer and pancreatic cancer, it was found that in the process of protein transfer from the endoplasmic reticulum to the Golgi body, the expression of related glycosylases such as Man1a1 was reduced, and the glycosylation process was blocked, so the N-connected hypermannosan was abnormally concentrated.[32–35] High mannoglycan participates in lysosomal pathways, collagen metabolism and other processes, leading to extracellular matrix (ECM) degradation and exacerbating the migration and invasion of cancer cells. High mannoglycan is of great significance for distinguishing normal tissues and cancer cells, and tracking the metastasis of cancer cells.[33] Clinical studies found that patients with low-expression of Man1a1 showed a shorter no-pathic period, and low Man1a1 expression was significantly negatively correlated with lymph node status, grade and distant metastasis.[36] Glycosylated proteomics study of renal transparent cell carcinoma found that high mannitre glycan accounted for 44.8% of the upregulated complete glycopeptide, while Man1a1 was

significantly lowered.[37] In our study, inducing reduced Man1a1 expression in obese mice, further supporting obesity can increase the risk of renal carcinoma, and semaglutide seems to reverse this process.

Ntn4 is a member of the neuron-directing factor family, which can promote the growth and elongation of neuronoids and participate in the axon-direction and cell migration of neurodevelopment. The study found that the expression of Ntn4 in liver cancer and breast cancer tissue is reduced, especially in breast cancer.[38,39] The low-expression of Ntn4 is significantly negatively correlated with the proliferation and metastasis of breast cancer, and the high expression of Ntn4 is a biomarker with a better survival rate for patients.[40] Single-gene Cox analysis shows that Ntn4 is also a protective factor for renal clear cell carcinoma (HR < 1).[40] Through flow cytometry, it is found that Ntn4 induces the cell cycle protein D1 to lower and increase stage G1 stage stagnation, reducing cell proliferation ability. Western blot analysis also shows that the expression of Ntn4 overexpress group apoptosis protein Bax and lyase caspase-3 increases, and the expression of anti-apoptosis protein Bcl-2 decreases. Overexpression of Ntn4 can induce renal clear cell cancer cell cycle stagnation and apoptosis, which is related to Ntn4 inhibits Wnt/β-catenin signaling in kidney cancer cells through GSK3β.[40]

We screened the low expression of Man1a1 and Ntn4 in KIRC tissue through bioinformatics methods, and in our obese mouse model, we also found that Man1a1 and Ntn4 were downgraded in the high-fat-induced obesity group, indicating that they may participate in the development of KIRC. Obesity can induce liver cancer, and semaglutide has a positive effect on improving liver cancer by regulating ITGAV, LAMC1, FABP5, and LPL proteins.[41] In the kidneys, semaglutide can increase the expression of Man1a1, Ntn4, and may be used as a new intervention target for the prevention and treatment of KIRC, which needs to be further verified in the population and cell level of renal clear cell cancer.

Although our study of the effect of semaglutide on KIRC is advanced and innovative, there are still many shortcomings in this experiment. We screened target proteins in obesity models and lack further verification in cancer tissues. After all, the development of cancer is a complex biological process. The variation of genes and the interaction of proteins complicate the carcinogenic mechanism. Therefore, this experiment was only a preliminary screening of targets for KIRC intervention, and our conclusions will be further verified in KIRC cells.

Conclusion

Semaglutide improved the weight, kidney structure and function of obesity-induced mice, improved glycolipid metabolism, and reduced inflammation and oxidative stress. And semaglutide could regulate the development of KIRC by up-adjusting the expression of Man1a1 and Ntn4.

Experimental Animal Ethics

All experiments and procedures were conducted in accordance with the Regulations on the Management of Laboratory Animals issued by the National Science and Technology Commission and were approved by the Animal Ethics Association of the Hebei General Hospital (Approval Number: 202332). The ARRIVE criteria were adopted in all animal trials.

The data involved in human research in this experiment came from the public database. According to the National Legislative Guide of the Measures for the Ethical Review of Life Sciences and Medical Research Involving the Human Body issued by China on February 18, 2023, we have been exempted from ethical review. The specific legislative details are as follows:

Article 32: If the use of human information data or biological samples to carry out the following circumstances involves human life science and medical research, does not cause harm to the human body and does not involve sensitive personal information or commercial interests, the ethical examination may be exempted to reduce the unnecessary burden on scientific researchers and promote the development of human life science and medical research.

(1) Using legally obtained public data or data generated by observation without interfering with public behavior.

(2) Using anonymous information data to carry out research.

Data Sharing Statement

Data supporting the findings of this study are available from the corresponding authors.

Funding

This study was supported by the Hebei Province Natural Science Foundation (H2022307026).

Disclosure

All authors declare that there is no conflict of interest in this study.

References

1. Piché ME, Tchernof A, Després JP. Obesity phenotypes, diabetes, and cardiovascular diseases. *Circ Res*. 2020;126(11):1477–1500. doi:10.1161/CIRCRESAHA.120.316101
2. Finucane MM, Stevens GA, Cowan MJ, et al. National, regional, and global trends in body-mass index since 1980: systematic analysis of health examination surveys and epidemiological studies with 960 country-years and 9·1 million participants. *Lancet*. 2011;377(9765):557–567. doi:10.1016/S0140-6736(10)62037-5
3. Lazarus E, Bays HE. Cancer and obesity: an obesity medicine association (OMA) clinical practice statement (CPS) 2022 *Obes Pillars*. 2022;3:100026. doi:10.1016/j.obpill.2022.100026
4. Decastro GJ, McKiernan JM. Epidemiology, clinical staging, and presentation of renal cell carcinoma. *Urol Clin N Am*. 2008;35(4):581–592. doi:10.1016/j.ucl.2008.07.005
5. Botero-Fonnegra C, Funes DR, Valera RJ, et al. Potential beneficial effects of bariatric surgery on the prevalence of kidney cancer: a national database study. *Surg Obes Relat Dis*. 2022;18(1):102–106. doi:10.1016/j.soard.2021.08.012
6. Pan X, Yue L, Ban J, et al. Effects of semaglutide on cardiac protein expression and cardiac function of obese mice. *J Inflamm Res*. 2022;15:6409–6425. doi:10.2147/JIR.S391859
7. Yue L, Chen S, Ren Q, et al. Effects of semaglutide on vascular structure and proteomics in high-fat diet-induced obese mice. *Front Endocrinol*. 2022;13. doi:10.3389/fendo.2022.995007
8. Niu S, Chen S, Chen X, et al. Semaglutide ameliorates metabolism and hepatic outcomes in an NAFLD mouse model. *Front Endocrinol*. 2022;13. doi:10.3389/fendo.2022.1046130
9. Ren Q, Chen S, Chen X, et al. An effective glucagon-like peptide-1 receptor agonists, semaglutide, improves sarcopenic obesity in obese mice by modulating skeletal muscle metabolism. *Drug Des Devel Ther*. 2022;16:3723–3735. doi:10.2147/DDDT.S381546
10. Chen X, Ma L, Gan K, et al. Phosphorylated proteomics-based analysis of the effects of semaglutide on hippocampi of high-fat diet-induced-obese mice. *Diabetol Metab Syndr*. 2023;15(1). doi:10.1186/s13098-023-01023-y
11. Chen X, Chen S, Ren Q, et al. Metabolomics provides insights into renoprotective effects of semaglutide in obese mice. *Drug Des Devel Ther*. 2022;16:3893–3913. doi:10.2147/DDDT.S383537
12. Sung H, Ferlay J, Siegel RL, et al. Global cancer statistics 2020: GLOBOCAN estimates of incidence and mortality worldwide for 36 cancers in 185 countries. *CA-Cancer J Clin*. 2021;71(3):209–249. doi:10.3322/caac.21660
13. Scelo G, Larose TL. Epidemiology and risk factors for kidney cancer. *J Clin Oncol*. 2018;36(36):3574–3581. doi:10.1200/JCO.2018.79.1905
14. Safiri S, Kolahi AA, Mansournia MA, et al. The burden of kidney cancer and its attributable risk factors in 195 countries and territories, 1990-2017. *Sci Rep*. 2020;10(1). doi:10.1038/s41598-020-70840-2
15. Lee JE, Nam CM, Lee SG, et al. The economic burden of cancer attributable to obesity in Korea: a population-based cohort study. *Eur J Cancer Care*. 2019;28. doi:10.1111/ecc.13084
16. Tracey KJ, Cerami A. Metabolic responses to cachectin/TNF. A brief review. *Ann NY Acad Sci*. 1990;587(1):325–331. doi:10.1111/j.1749-6632.1990.tb00173.x
17. Bukavina L, Bensalah K, Bray F, et al. Epidemiology of renal cell carcinoma: 2022 update. *Eur Urol*. 2022;82(5):529–542. doi:10.1016/j.eururo.2022.08.019
18. Lan N, Lu Y, Zhang Y, et al. FTO - A common genetic basis for obesity and cancer. *Front Genet*. 2020;11. doi:10.3389/fgene.2020.559138
19. Brennan P, McKay J, Moore L, et al. Obesity and cancer: Mendelian randomization approach utilizing the FTO genotype. *Int J Epidemiol*. 2009;38(4):971–975. doi:10.1093/ije/dyp162
20. Tamayo-Trujillo R, Ruiz-Pozo VA, Cadena-Ullauri S, et al. Molecular mechanisms of semaglutide and liraglutide as a therapeutic option for obesity. *Front Nutr*. 2024;11. doi:10.3389/fnut.2024.1398059
21. Hunter CA, Kartal F, Koc ZC, et al. Mitochondrial oxidative phosphorylation is impaired in TALLYHO mice, a new obesity and type 2 diabetes animal model. *Int J Biochem Cell B*. 2019;116:105616. doi:10.1016/j.biocel.2019.105616
22. Chen Y, Gong Y, Zou J, et al. Single-cell transcriptomic analysis reveals transcript enrichment in oxidative phosphorylation, fluid sheer stress, and inflammatory pathways in obesity-related glomerulopathy. *Genes Dis*. 2024;11. doi:10.1016/j.gendis.2023.101101
23. Gross B, Staels B. PPAR agonists: multimodal drugs for the treatment of type-2 diabetes. *Best Pract Res Clin Endocrinol Metab*. 2007;21(4):687–710. doi:10.1016/j.beem.2007.09.004
24. Nahlé Z. PPAR trilogy from metabolism to cancer. *CURR OPIN CLIN NUTR*. 2004;7(4):397–402. doi:10.1097/01.mco.0000134360.30911.bb
25. Wagner N, Wagner KD. Pharmacological utility of PPAR modulation for angiogenesis in cardiovascular disease. *Int J mol Sci*. 2023;24(3):2345. doi:10.3390/ijms24032345
26. Hu N, Chen C, Wang J, et al. Atorvastatin ester regulates lipid metabolism in hyperlipidemia rats via the PPAR-signaling pathway and HMGCR expression in the liver. *Int J mol Sci*. 2021;22(20):11107. doi:10.3390/ijms222011107
27. Li H, Jia Y, Weng D, et al. Clostridium butyricum inhibits fat deposition via increasing the frequency of adipose tissue-resident regulatory T cells. *Mol Nutr Food Res*. 2022;66. doi:10.1002/mnfr.202100884
28. Shao X, Liu L, Zhou Y, et al. High-fat diet promotes colitis-associated tumorigenesis by altering gut microbial butyrate metabolism. *Int J Biol Sci*. 2023;19(15):5004–5019. doi:10.7150/ijbs.86717
29. Tanaka T, Kono T, Terasaki F, et al. Thiamine prevents obesity and obesity-associated metabolic disorders in OLETF rats. *J Nutr Sci Vitaminol*. 2010;56(6):335–346. doi:10.3177/jnsv.56.335

30. Qi Q, Li J, Yu B, et al. Host and gut microbial tryptophan metabolism and type 2 diabetes: an integrative analysis of host genetics, diet, gut microbiome and circulating metabolites in cohort studies. *Gut*. 2022;71(6):1095–1105. doi:10.1136/gutjnl-2021-324053
31. Lischka J, Schanzer A, Baumgartner M, et al. Tryptophan metabolism is associated with BMI and adipose tissue mass and linked to metabolic disease in pediatric obesity. *Nutrients*. 2022;14(2):286. doi:10.3390/nu14020286
32. Milde-Langosch K, Karn T, Schmidt M, et al. Prognostic relevance of glycosylation-associated genes in breast cancer. *Breast Cancer Res Tr*. 2014;145(2):295–305. doi:10.1007/s10549-014-2949-z
33. Hu Y, Pan J, Shah P, et al. Integrated proteomic and glycoproteomic characterization of human high-grade serous ovarian carcinoma. *Cell Rep*. 2020;33(3):108276. doi:10.1016/j.celrep.2020.108276
34. Park DD, Phoomak C, Xu G, et al. Metastasis of cholangiocarcinoma is promoted by extended high-mannose glycans. *Proc Natl Acad Sci U S A*. 2020;117(14):7633–7644. doi:10.1073/pnas.1916498117
35. Park HM, Hwang MP, Kim YW, et al. Mass spectrometry-based N-linked glycomic profiling as a means for tracking pancreatic cancer metastasis. *Carbohyd Res*. 2015;413:5–11. doi:10.1016/j.carres.2015.04.019
36. Legler K, Rosprim R, Karius T, et al. Reduced mannosidase MAN1A1 expression leads to aberrant N-glycosylation and impaired survival in breast cancer. *Br J Cancer*. 2018;118(6):847–856. doi:10.1038/bjc.2017.472
37. Lih TM, Cho KC, Schnaubelt M, et al. Integrated glycoproteomic characterization of clear cell renal cell carcinoma. *Cell Rep*. 2023;42(5):112409. doi:10.1016/j.celrep.2023.112409
38. Vennela J, Pottakkat B, Vairappan BS, et al. Hepatic expression of NTN4 and its receptors in patients with hepatocellular carcinoma. *Asian Pac J Cancer Prev*. 2023;24. doi:10.31557/APJCP.2023.24.12.4285
39. Yi L, Lei Y, Yuan F, et al. NTN4 as a prognostic marker and a hallmark for immune infiltration in breast cancer. *Sci Rep*. 2022;12(1). doi:10.1038/s41598-022-14575-2
40. Ke S, Guo J, Wang Q, et al. Netrin family genes as prognostic markers and therapeutic targets for clear cell renal cell carcinoma: netrin-4 acts through the Wnt/β-Catenin signaling pathway. *Cancers*. 2023;15(10):2816. doi:10.3390/cancers15102816
41. Liu Y, Chen S, Zhen R. Effect of Semaglutide on high-fat-diet-induced liver cancer in obese mice. *J Proteome Res*. 2024;23(2):704–717. doi:10.1021/acs.jproteome.3c00498